Supporting Information for:

Illuminating Cisplatin-induced Ferroptosis in Non-Small-Cell Lung Cancer with *Biothiols-Activable* Fluorescent/ Photoacoustic Bimodal Probes

Li Xu [a, #], Hongwen Liu [b #], Yi Kong [a], Lingyun Li [b], Jia Li [b], Kang Li [a], Shuzhi Liang [a], and Bolin Chen [a, *]

[a] The Second Department of Thoracic Oncology, Hunan Cancer Hospital/the Affiliated Cancer Hospital of Xiangya School of Medicine, Central South University, Changsha 410013, Hunan Province, P.R. China

[b] Key Laboratory of Light Energy Conversion Materials of Hunan Province College, College of Chemistry and Chemical Engineering, Hunan Normal University, Changsha 410081, P. R. China.

[#] These authors contributed equally.

Corresponding Author

Bolin Chen*, Email: chenbolin@hnca.org.cn

Table of Contents

1. Experimental procedures

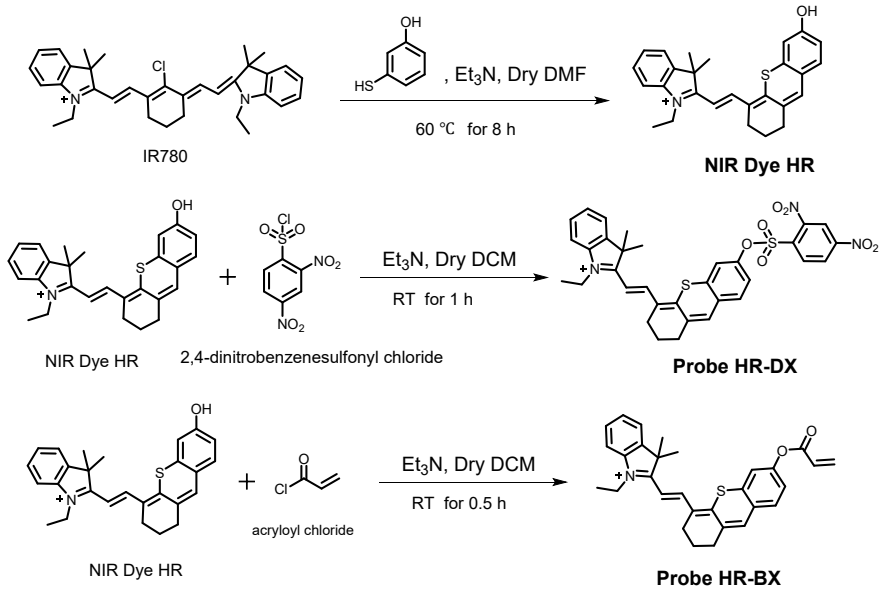

Scheme S1. The synthetic route of **HR-DX** and **HR-BX**.

EXPERIMENTAL SECTION

Materials and Measurements. All reagents and extra dry solvents were purchased from Admas (Shanghai, China), and used without further purification. The ultrapure water for aqueous solutions was prepared through a Millipore Milli-Q water purification system (Billerica, MA, USA), and pH determination was performed on a Mettler-Toledo Delta 320 pH meter. Thin layer chromatography analysis was done on silica gel plates, and column chromatography was conducted over silica gel (mesh 200-300), both of which were purchased from Qingdao Ocean Chemicals (China). ^{1}H and ^{13}C NMR spectra were proved on a Bruker DRX-400 spectrometer operating at 400 and 110 MHz with chemical shifts reported as ppm (TMS as internal standard). High resolution mass spectra (HRMS) were proved on Bruker MicroTOF-QII massinstrument (ESI). UV-Vis absorption spectra were recorded with a UV-3600 spectrophotometer (Shimadzu Corporation, Japan). All fluorescence intensity measurements *in vitro* were tested on a Edinburgh Instruments F-S5 fluorescence spectrometer with a 1 cm standard quartz cell. Cell Counting MTT assay (CCK-8) was purchased from Shanghai Beyotime Biotechnology Company (China). Fluorescence images of cells were obtained using a Nikon A1 plus

confocal microscope (Nikon, Japan).

Spectroscopic Measurements. Probe **HR-DX** and **HR-BX** were dissolved in DMSO to prepare stock solutions of 25 μM, which were diluted in PBS buffered solutions to form 20% DMSO containing aqueous samples of 5 μM probes for absorption and fluorescence spectral measurements. Different concentrations of Cys, Hcy, GSH, and H_2S were treated with 5 μM probes in PBS containing 20% DMSO for spectra titrations. The absorption spectra were measured during a range of 800-400 nm, and the fluorescence spectra were recorded at excitation wavelength of 730 nm. Various potential interferents were used to carry out the selectivity and competition experiments. pH effects were tested in a pH range of 4-9. And the time of fluorescence response were recorded every two minutes during 0-60 min.

Cytotoxicity Assay. The cell cytotoxicity of **HR-DX** and **HR-BX** was measured by the MTT assay. Generally, HepG2 and A549 cells were cultured in 96-well plates at 6×10^3 cells in 100 μL culture medium per well and incubated at 37 ℃ for 20 h. Then the medium was replaced with medium composed of **HR-DX** or **HR-BX** with the concentration of 2, 4, 6, 8 and 10 μM, and co-incubated for 4 h before replacing with fresh culture medium. After incubation for 24 h, the cells were added with MTT (10 μL) for 2 h. The absorbance at 490 nm of each well was determined via a microplate reader, and the following formula was used to evaluate the cell viability: Cell viability ratio (%) = $(OD_{Sample} - OD_{PBS})/(OD_{Blank} - OD_{PBS}) \times 100\%$.

Cell Culture and Fluorescence Imaging. Living cancer cells (A549 and HepG2) were obtained from the Biomedical Engineering Center of Hunan University (Hunan Changsha, China) and cultured in DMEM (Dulbecco's modified Eagle's medium) supplemented with 10% FBS (Fetal bovine serum) at 37 ℃ under a 5% CO_2 atmosphere. For imaging of endogenous or exogenous biothiols, A549 and HepG2 cells were rinsed with a DPBS buffer (pH 7.4) for three times, and eight groups were treated without or pretreated with NEM and further with 20 μM biothiols (Cys, Hcy, 0.5 mM GSH and H_2S) for 0.5 h, respectively. Each group was then incubated with probe (5 μM) **HR-DX** or **HR-BX** for another 0.5 h before imaging. For dose-dependent imaging of endogenous biothiols, A549 and HepG2 cells were rinsed with a DPBS buffer (pH 7.4) for three times, and eight groups were treated with **HR-DX** or **HR-BX** (5 μM) for 5, 10, …, 30 and 40 min before imaging. For studying of erastin induced ferroptosis, A549 cells were rinsed with a DPBS buffer (pH 7.4) for three times, and each group were treated with erastin (2, 4, 6, 8, 10 μM) for 4 h, further with 5 μM probes (**HR-DX** or **HR-BX**) for 0.5 h, respectively, before imaging. For another group, the A549 cells were rinsed with a DPBS buffer (pH 7.4) for three times, and each group were treated with 8 μM erastin for 4 h, further with 10 μM Ferrostatin-1 for another 2 h before added 5 μM probes (**HR-DX** or **HR-BX**) for co-incubating for 30 min, respectively, before imaging. Other groups followed the similar operation. All cells were rinsed three times with DPBS, after which the fluorescence images were obtained using Nikon A1 plus confocal fluorescence microscope (Nikon, Japan) with 640 nm excitation for the NIR channel (680–780 nm).

***In vivo* Imaging.** C57BL/6 mice (female, 8 weeks), inoculated with A549 subcutaneous tumor, were ordered from Slake Jingda Experimental Animal Co., Ltd (Hunan). Mix A549 cancer cells (about 5×10^5) with matrix gel and inject them subcutaneously into mice, tumor formation could be observed about a week later. The above tumor-bearing mice were adopted to the fluorescence and photoacoustic imaging experiments in vivo. 20 μL 20 μM **HR-DX** or **HR-BX** was injected into the left axillary and right axillary tumor area of the A549 mouse model, while the other mouse was firstly injected 40 μL 5 mM NEM in the right axillary waiting for 30

min and injected **HR-DX** or **HR-BX** directly in left and right area. At specific time intervals, the mice were subjected to anesthesia using 2.5% isoflurane in an oxygen environment. Subsequently, whole-body NIR fluorescence images were acquired employing an NIR in vivo master system, utilizing a 715 nm laser (100 mW/cm^2) and a ICG filter (750-850 nm). The exposure time was set to 400 ms for optimal imaging quality. During photoacoustic imaging, mice are placed on their back in a water bath at 32 °C and anesthesia and oxygen are administered through a respirator. Using back projection and linear regression multispectral demixing techniques reconstructed PA images. The specific photoacoustic imaging parameters are as followed: scanning area: the cross section of right axillary tumor (30.26 mm-36.99 mm, x=4.9 mm, y=14 mm); Speed of sound: 10; low-pass filter range: 50.0 kHz-6.5 MHz; Laser energy: 47 mJ (735 nm); Pulse repetition rate: 1; Image size: 25 mm (res:75 μm);

For fluorescent imaging, the SBR was calculated according to the following formula: SBR= (the signal intensity within a defined range -the signal strength at 0 min of normal tissue)/ the signal strength at 0 min of normal tissue.

Due to the complexity of PA imaging operations, it is very difficult to obtain the signal intensity at 0 min point of injection of the probes. And to maintain consistency, we set the acquisition time points of the two imaging modes to be the same. Thus, for PA imaging, the SBR was calculated according to the following formula: SBR= the signal intensity within a defined range / the signal strength at 10 min of normal tissue.

Live cells and live mouse experiments were in agreement with institutional animal care and use regulations, according to protocol No. SYXK (Xiang) 2020-0012, approved by Laboratory Animal Center of Hunan.

Table S1. Comparison of fluorescent probes for biothiols with the present probe **HR-DX** and **HR-BX**.

Probe	Analyte	$\lambda_{abs}/\lambda_{em}$ (nm)	LOD	Linear range	Response time	Enhance-ment	Applications
[1]	Cys	340/443	0.16 μM	0-35 μM	14 min	25-fold	Imaging in PC12 cells and living mouse brain
[2]	Cys	460/515	0.18 μM	0-100 μM	30 min	35-fold	Imaging in A549 cells
[3]	Cys	660/851	10.6 nM	0-8 μM	3 min	-	Fluorescent and Photoacoustic imaging in LO2 and HepG2 cells, tumor bearing mice
[4]	Cys	645/760	0.07 μM	3-100 μM	30 min	-	Fluorescent and Photoacoustic imaging in cells, tumor bearing mice
[5]	GSH	410/510 to 350/460	245 nM	0-6 mM	-	-	Imaging of GSH dynamics in the nucleoli in the cell cycle process
[6]	GSH	530/587 to 420/505	-	-	10 s	-	Quantitative and real-time imaging in living cells
[7]	GSH	594/613 to 527/544	-	-	-	-	Real-time quantitative imaging of GSH fluctuation in living cells
[8]	GSH	892/928	80 nM	0-20 μM	60 min	16-fold	NIR-II imaging in living cells

							and tumor bearing mice
[9]	GSH	710/736	-	-	-	-	Ratiometric quantitative and real-time imaging in living cells and mice
[10]	GSH	-	-	-	-	-	Quantification of redox potential and GSH concentration
[11]	Hcy	488/550	0.084 ppm	-	5 min	-	Monitoring Hcy level in plasma from the GBM-xenograft mouse model
[12]	Hcy	345/456	18 nM	0-10 μM	60 min	-	Monitoring Hcy level in serum, living cells, and atherosclerosis model mice
[13]	Hcy	568/654	3.7 nM	0-8 μM	30 min	357-fold	Monitoring Hcy in type 2 diabetes mellitus and Alzheimer's disease
[14]	Cys Hcy	425/495	49 nM 51 nM	0-10 μM	3 min		Imaging in cells and mouse liver slice
[15]	Cys Hcy GSH	537/675	68 nM 69 nM 52 nM	0-60 μM	150 s 250 s 140s	36-fold	Revealing the negative relationship between the level of thiols and the occurrence of

							epilepsy
[16]	Cys Hcy GSH	458/528	78.8 nM 90.5 nM 86.4 nM	0-4.5 μM 0-4.5 μM 0-5 μM	60 s	180-fold	Imaging in cells and mouse tissues
[17]	Cys Hcy GSH	494/557	70 nM 49 nM 62 nM	0-10 μM	10 s	82-fold	Imaging in HeLa cells and labeling sulfhydryl-containing proteins
[18]	Cys Hcy GSH	541/713	27 nM 74 nM 55 nM	0-20 μM	9 min 27 min 20 min	65-fold 49-fold 57-fold	Imaging changes of biothiols in vivo in the brains of mice during CIRI
[19]	Cys Hcy	580/620 to 445/540	22 nM 23 nM	2-8 μM 4-12 μM	5 min 10 min	163-fold 125-fold	Visualizing mitochondrial biothiols in living cells and Daphnia magna model
[20]	Cys Hcy GSH	397/503 375/467 500/568	0.2 nM 0.7 nM 1 nM	0-30 μM 0-30 μM 0-10 μM	15 min	740-fold 457-fold 115-fold	Visualizing endogenous Hcy, Cys, GSH, and their transformation in living cells
[21]	Cys Hcy GSH	396/495 396/495 505/565	106 nM 82 nM 57 nM	0-30 μM 0-30 μM 0-15 μM	25 min 25 min 20 min	119-fold 130-fold 288-fold	Discrimination of different biothiols in cells and zebra fish
[23]	Cys Hcy	690/712	0.11 μM 0.09 μM	0-20 μM	5 min	18.9-fold	Cell screening, exogenous biothiols imaging, and

	GSH		0.07 μM				monitoring drug induced biothiols fluctuations.
This Work	Cys	730/765	2.4 μM	0-60 μM	15 min	4-fold	NIR fluorescent/photoacoustic bimodal imaging of ferroptosis in NSCLC.
This Work	GSH	730/765	6.1 μM	0-80 μM	30 min	25-fold	NIR fluorescent/photoacoustic bimodal imaging of ferroptosis in NSCLC.

1. Zhang, Y.; Wang, X.; Bai, X.; Li, P.; Su, D.; Zhang, W.; Zhang, W.; Tang, B. *Anal. Chem.* **2019**, *91*, 8591–8594.
2. Karakuş, E.; Sayar, M.; Dartar, S.; Kaya, B. U.; Emrullahoğlu, M. *Chem. Commun.* **2019**, *55*, 4937–4940.
3. Chen, Z.; Wang, B.; Liang, Y.; Shi, L.; Cen, X.; Zheng, L.; Liang, E.; Huang, L.; Cheng, K. *Anal. Chem.* **2022**, *94*, 10737–10744.
4. Gu, Q.-S.; Yang, Z.-C.; Chao, J.-J.; Li, l.; Mao, G.-J.; Xu, F.; Li, C.-Y. *Anal. Chem.* **2023**, *95*, 12478–12486.
5. Khatun, S.; Yang, S.; Zhao, Y. Q.; Lu, Y.; Podder, A.; Zhou, Y.; Bhuniya, S. *Anal. Chem.* **2020**, *92*, 10989–10995.
6. Tian, M.; Liu, X.-Y.; He, H.; Ma, X.-Z.; Liang, C.; Liu, Y.; Jiang, F.-L. *Anal. Chem.* **2020**, *92*, 10068–10075.
7. Liu, H.; Song, W.; Zhang, S.; Chan, K. S.; Guo Z.; Shen, Z. *Chem. Sci.* **2020**, *11*, 8495–8501.
8. Pan,Y.; Lei, S.; Zhang, J.; Qu, J.; Huang, P.; Lin, J. *Anal. Chem.* **2021**, *93*, 17103–17109.
9. Li, N.; Wang, T.; Wang, N.; Fan, M.; Cui, X. *Angew. Chem. Int. Ed.* **2022**, e202217326
10. Emmert, S.; Quargnali, G.; Thallmair, S.; Rivera-Fuentes, P. *Nat. Chem.* **2023**. https://doi.org/10.1038/s41557-023-01249-3.
11. Kim, Y.; An, J. M.; Kim, J.; Chowdhury, T.; Yu, H. J.; Kim, K.-M.; Kang, H.; Park, C.-K.; Joung, J. F.; Park, S.; Kim, D. *Anal. Chim. Acta* **2022**, *1202*, 339678.
12. Wei, F.; Ding, Y.; Ou, J.; Chen, X.; Li, L.; Zhou, Q.; Chen, Q.; Wang, Q.; Feng, Y.; Meng, X. *Anal. Chem.* **2023**, *95*, 9173–9181.
13. Yin, G.; Gan, Y.; Jiang, H.; Yu, T.; Liu, M.; Zhang, Y.; Li, H.; Yin, P.; Yao, S. *Anal. Chem.* **2023**, *95*, 8932–8938.
14. Cheng, T.; Huang, W.; Gao, D.; Yang, Z.; Zhang, C.; Zhang, H.; Zhang, J.; Li, H.; Yang, X.-F. *Anal. Chem.* **2019**, *91*, 10894–10900.
15. Yang, Y.; Zhang, Y.; Ma, M.; Liu, H.; Ge, K.; Zhang, C.; Jin, M.; Liu, D.; Wang, S.; Yin, C.; Zhang, J. *Anal. Chem.* **2022**, *94*, 14443–14452.
16. Zhang, Y.; Zhang, N.; Wang, S.; Zan, Q.; Wang, X.; Yang, Q.; Yu, X.; Dong, C.; Fan, L. *Analyst* **2022**, *147*, 1695–1701.

17. Zheng, S.; Peng, J.; Jiang, L.; Gu, H.; Wang, F.; Wang, C.; Lu, S.; Chen, C. *Sens. Actuators B: Chem.* **2022**, *367*, 132148.
18. Yang, Y.; Ma, M.; Shen, L.; An, J.; Kim, E.; Liu, H.; Jin, M.; Wang, S.; Zhang, J.; Kim, J. S.; Yin, C. *Angew. Chem.Int. Ed.* **2023**, e202310408.
19. Yang, M.; Fan, J.; Sun, W.; Du, J.; Peng, X. *Anal. Chem.* **2019**, *91*, 12531–12537.
20. Yin, G.; Niu, T.; Yu, T.; Gan, Y.; Sun, X.; Yin, P.; Chen, H.; Zhang, Y.; Li, H.; Yao, S. *Angew. Chem.Int. Ed.* **2019**, *58*, 4557–4561.
21. Wang, X.-B.; Li, H.-J.; Liu, C.; Hu, Y.-X.; Li, M.-C.; Wu, Y.-C. *Anal. Chem.* **2021**, *93*, 2244–2253.
22. Zhang, Y.; Liu, C.; Sun, W.; Yu, Z.; Su, M.; Rong, X.; Wang, X.; Wang, K.; Li, X.; Zhu, H.; Yu, M.; Sheng, W.; Zhu, B. *Anal. Chem.* **2022**, *94*, 7140–7147.
23. Gong, Y.; Wang, P.; Zhai, H.; Xiao, Y.; Wang, Q.; Ma, N.; Zhang, G.; Zhang, H., *Anal. Chem.* **2024**, 96, 3, 1009–1018

2. Supplementary figures

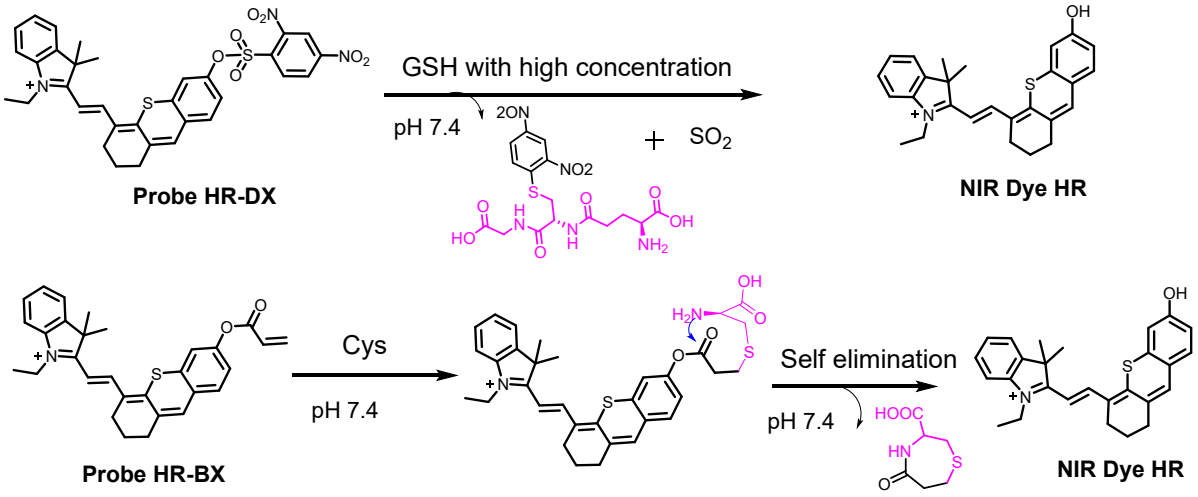

Scheme S2. Design of the probes, their response mechanism with GSH or Cys under physiological condition.

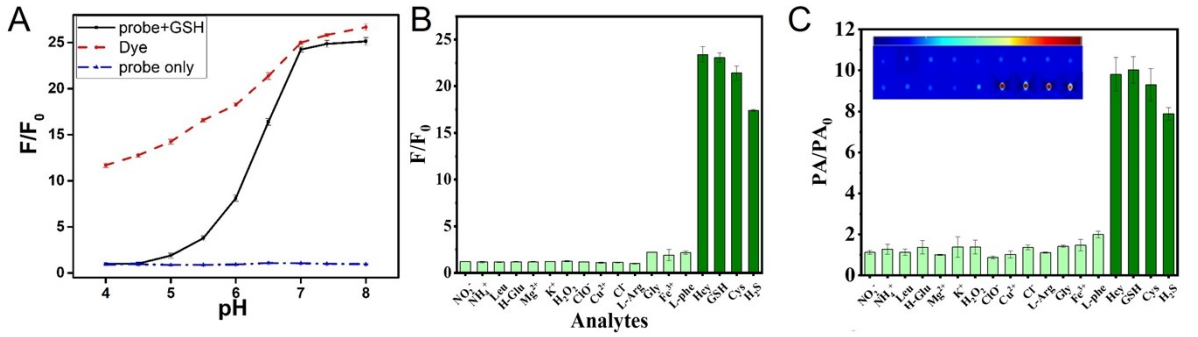

Fig. S1. Response test of the probe HR-DX (5 μM) to 200 μM GSH in PBS/DMSO (v/v=8/2, pH=7.4) at 37 °C. (A) Fluorescent change of HR-DX or HR at 765 nm in buffer solutions with different pH from 4.0 to 8.0; (B) Fluorescence change of HR-DX at 765 nm in the presence of GSH (200 μM) and other disturbing species including usual ions and ROS/RNS, or others biothls, and (C) corresponding PA signal change at 735 nm and images of PA in tube (insert); The concentration of NO_2, NH_4^+, Leu, H-Glu, L-Arg, Gly, and L-Phe is 1 mM; The concentration of Mg^{2+}, Na^+, K^+ and Cl^- is 10 mM; The concentration of Cu^{2+} and Fe^{3+} is 0.1 mM; The concentration of H_2O_2 and ClO^- is 100 and 10 μM, respectively; The concentration of Hcy, GSH, Cys and NaHS is 200 μM. λ_{ex} = 730 nm and λ_{em} = 765 nm for fluorescence spectra.

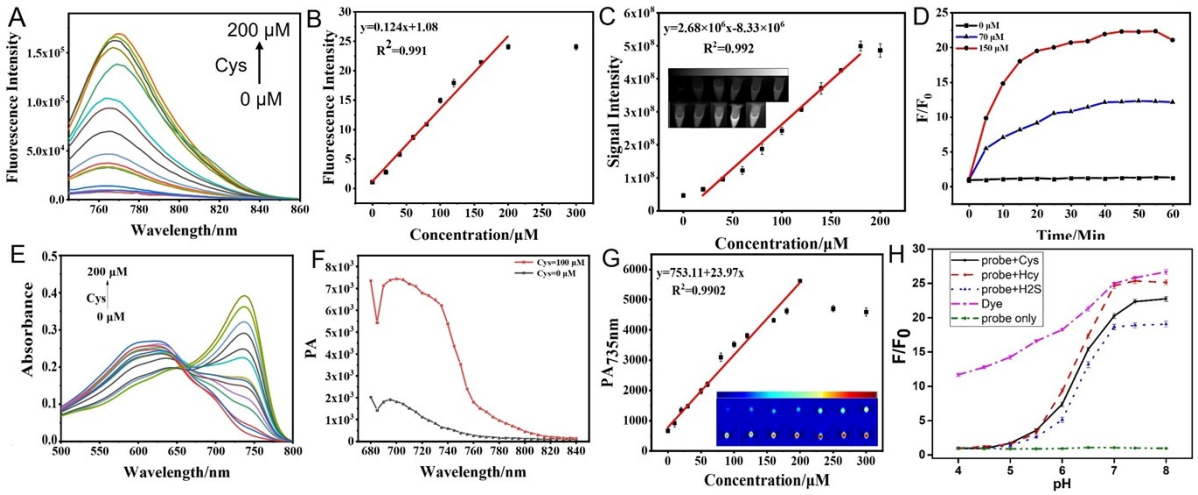

Fig. S2. Response test of the probe HR-DX (5 μM) to Cys in PBS/DMSO (v/v=8/2, pH=7.4) at 37 °C. (A) Fluorescence spectra of HR-DX in response Cys with concentrations of 0-200 μM; (B) Fluorescence responses and corresponding linear responses of HR-DX at 765 nm toward Cys with concentrations of 0-200 μM; (C) Responses test using in vivo imaging system and corresponding linear responses of HR-DX toward Cys with concentrations of 0-200 μM, insert: near infrared fluorescent imaging of HR-DX for Cys; (D) Time-dependent fluorescence responses at 765 nm of HR-DX to Cys; (E) Absorption spectra of HR-DX in response to 0-200 μM Cys; (F) PA spectrum of HR-DX in the absence and present of 100 μM Cys; (G) The image of PA and the corresponding line relationship of HR-DX after incubation with different concentrations of Cys (0-300 μM; (H) Fluorescence spectra of HR-DX at 765 nm in buffer solutions with different pH from 4.0 to 8.0; λ_{ex} = 730 nm and λ_{em} = 765 nm for fluorescence spectra, λ_{ex} =715 nm and λ_{em} = 750-820 nm for fluorescent imaging, and λ_{ex} =735 nm for PA imaging.

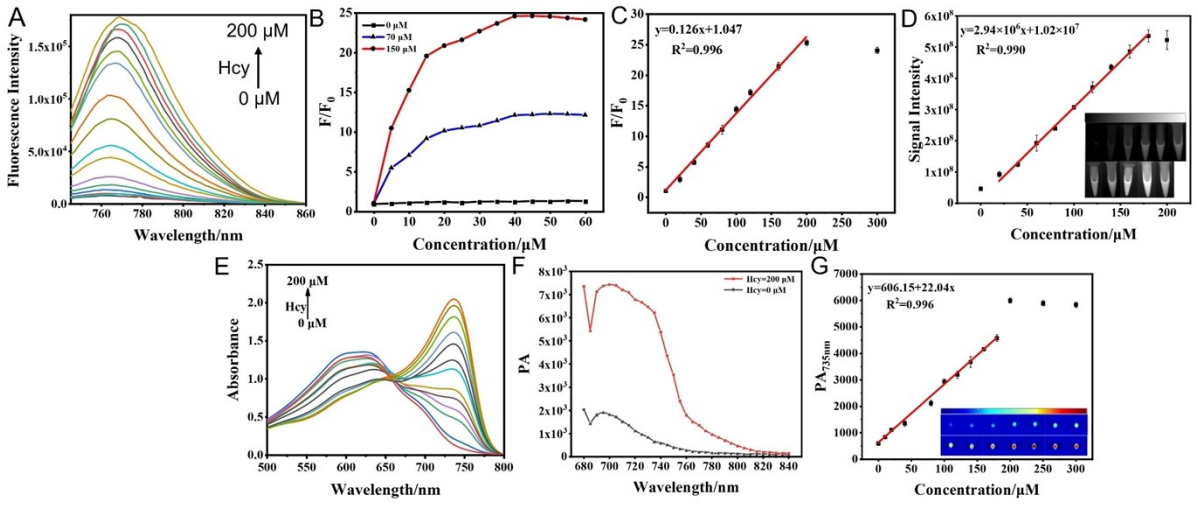

Fig. S3. Response test of the probe HR-DX (5 μM) to Hcy in PBS/DMSO (v/v=8/2, pH=7.4) at 37 °C. (A) Fluorescence spectra of HR-DX in response Hcy with concentrations of 0-200 μM; (B) Fluorescence responses and corresponding linear responses of HR-DX at 765 nm toward Hcy with concentrations of 0-200 μM; (C) Responses test using in vivo imaging system and corresponding linear responses of HR-DX toward Hcy with concentrations of 0-200 μM, insert: near infrared fluorescent imaging of HR-DX for Hcy; (D) Time-dependent fluorescence responses at 765 nm of HR-DX to Hcy; (E) Absorption spectra of HR-DX in response to 0-200 μM Hcy; (F) PA spectrum of HR-DX in the absence and present of 200 μM Hcy; (G) The image of PA and the corresponding line relationship of HR-DX after incubation with different

concentrations of Hcy (0-300 μM); λ_{ex} = 730 nm and λ_{em} = 765 nm for fluorescence spectra, λ_{ex} =715 nm and λ_{em} = 750-820 nm for fluorescent imaging, and λ_{ex} =735 nm for PA imaging.

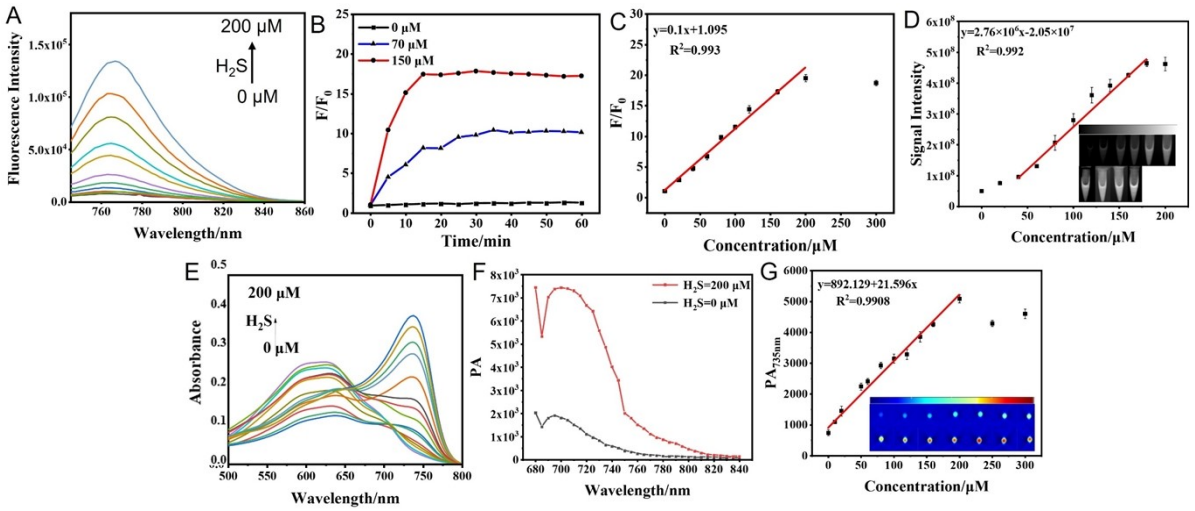

Fig. S4. Response test of the probe HR-DX (5 μM) to H_2S in PBS/DMSO (v/v=8/2, pH=7.4) at 37 °C. (A) Fluorescence spectra of HR-DX in response H_2S with concentrations of 0-200 μM; (B) Fluorescence responses and corresponding linear responses of HR-DX at 765 nm toward H_2S with concentrations of 0-200 μM; (C) Responses test using in vivo imaging system and corresponding linear responses of HR-DX toward H_2S with concentrations of 0-200 μM, insert: near infrared fluorescent imaging of HR-DX for H_2S; (D) Time-dependent fluorescence responses at 765 nm of HR-DX to H_2S; (E) Absorption spectra of HR-DX in response to 0-200 μM H_2S; (F) PA spectrum of HR-DX in the absence and present of 200 μM H_2S; (G) The image of PA and the corresponding line relationship of HR-DX after incubation with different concentrations of H_2S (0-300 μM); λ_{ex} = 730 nm and λ_{em} = 765 nm for fluorescence spectra, λ_{ex} =715 nm and λ_{em} = 750-820 nm for fluorescent imaging, and λ_{ex} =735 nm for PA imaging.

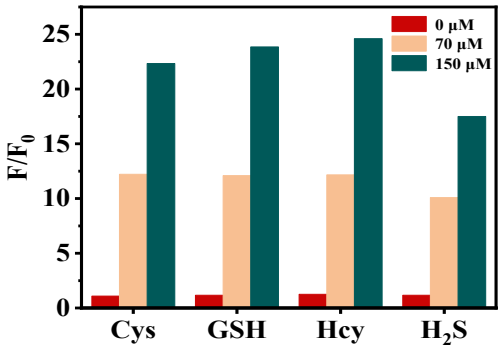

Fig. S5. Response test of the probe HR-DX (5 μM) to biothiols in PBS/DMSO (v/v=8/2, pH=7.4) at 37 °C. The results demonstrated that HR-DX shows similar response performance to GSH, Hcy and Cys, but the 150 μM H_2S may induce the destruction of the probe via nucleophilic addition reaction.

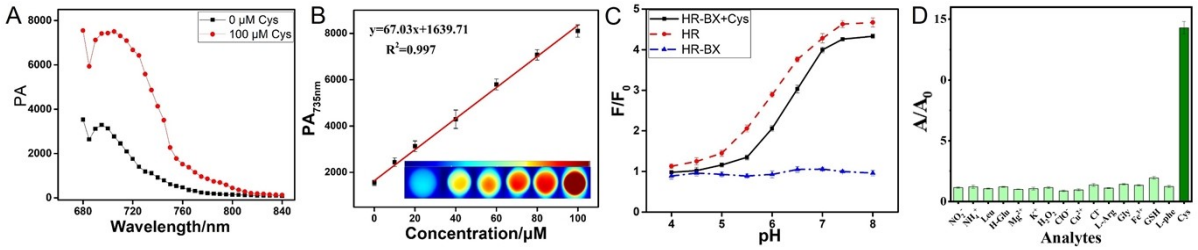

Fig. S6. Response test of the probe HR-BX (5 μM) to Cys in PBS/DMSO (v/v=8/2, pH=7.4) at 37 °C. (A) PA spectrum of HR-BX in the absence and present of 100 μM Cys; (B) The images of PA imaging and the corresponding line relationship of HR-BX after incubation with different concentrations of Cys (0-100 μM); (C) Fluorescence spectra of HR-DX at 765 nm in buffer solutions with different pH from 4.0 to 8.0; (D) Absorption changes of HYD-BX at 735 nm in the presence of Cys (100 μM) and other disturbing species including usual ions and ROS/RNS, or others biothls in tube; λ_{ex} = 730 nm and λ_{em} = 765 nm for fluorescence spectra, and λ_{ex} = 735 nm for PA imaging.

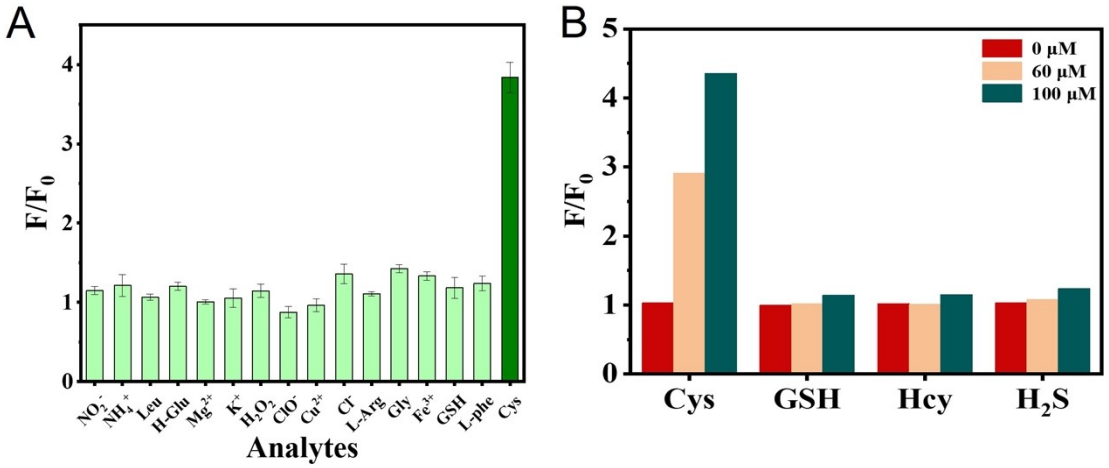

Fig. S7. Selective test of the probe HR-BX (5 μM) to Cys in PBS/DMSO (v/v=8/2, pH=7.4) at 37 °C. (A) Fluorescent change of HR-BX at 765 nm in the presence of Cys (100 μM) and other disturbing species including usual ions and ROS/RNS, or others biothls in tube; (B) Fluorescence change of HYD-BX at 765 nm in the presence of Cys and other biothiols (GSH, Hcy and H_2S) at (0, 60 and 100 μM); λ_{ex} = 730 nm and λ_{em} = 765 nm.

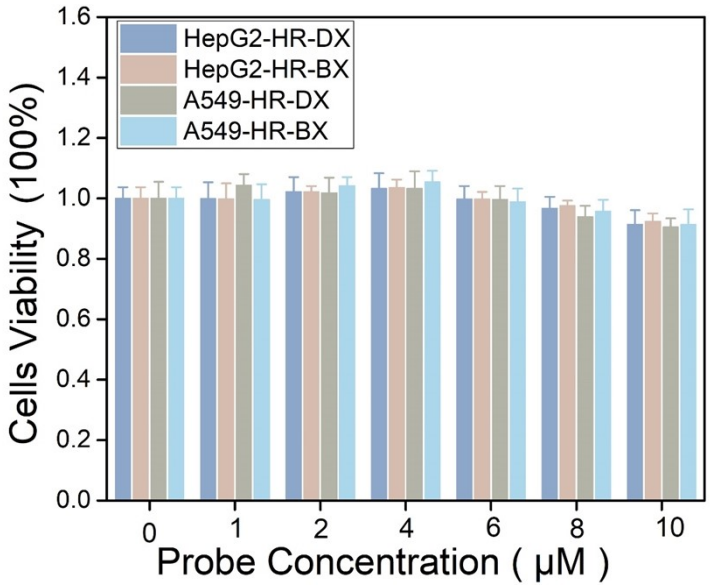

Fig. S8. HR-DX and HR-BX against HepG2 and A549 cells as determined by MTT assay. HepG2 or A549 cells were treated with HR-BX (0-10 μM) or HR-DX (0-10 μM) for 4 h, then incubated in fresh culture medium for 24 h before added MTT.

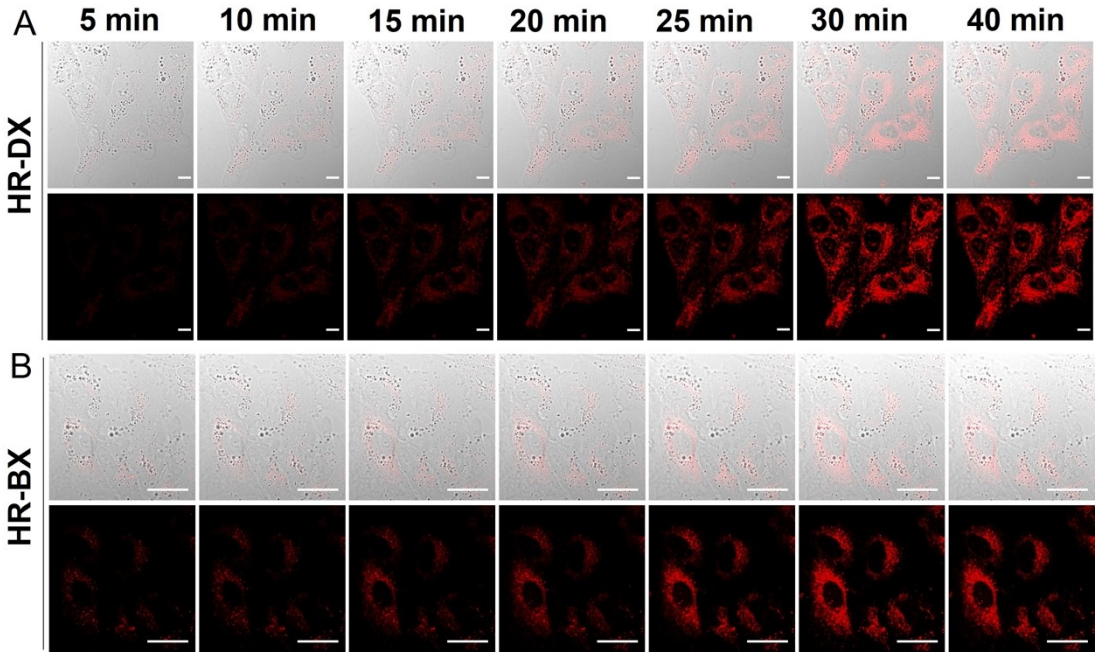

Fig. S9. Fluorescent Real-time imaging of endogenous GSH in A549 cells with probes (5 μM). Fluorescent imaging in A549 cells incubated with (A) HR-DX or (B) HR-BX, the images were collected every 5 minutes. λ_{ex} =640 nm, λ_{em} =680-780 nm, scale bar: 20 μm.

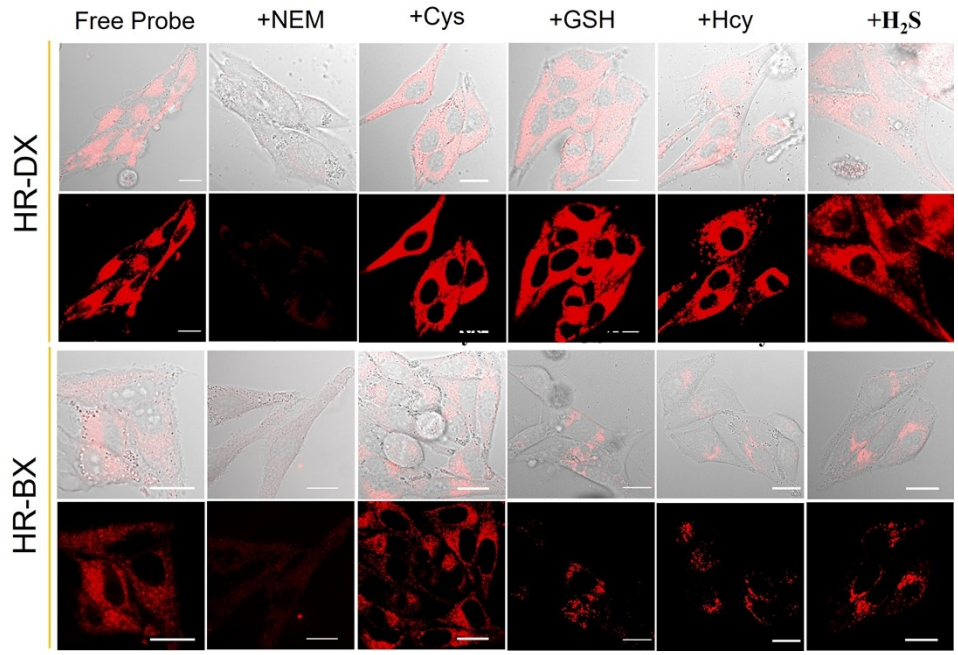

Fig. S10. Fluorescent imaging of HepG2 cells with HR-DX or HR-BX (5 μM), respectively. (A and C) Selectivity test of HR-DX or HR-BX via fluorescent imaging in HepG2 cells. The cells were incubated with the probe, or pretreated with 1 mM NEM for 30 min then co-incubated with 100 μM Cys, 1000 μM GSH, 100 μM Hcy, or 100 μM NaHS, respectively, for another 30 min before added HYD-BX for further co-incubation. λ_{ex} =640 nm, λ_{em} =680-780 nm, scale bar: 20 μm.

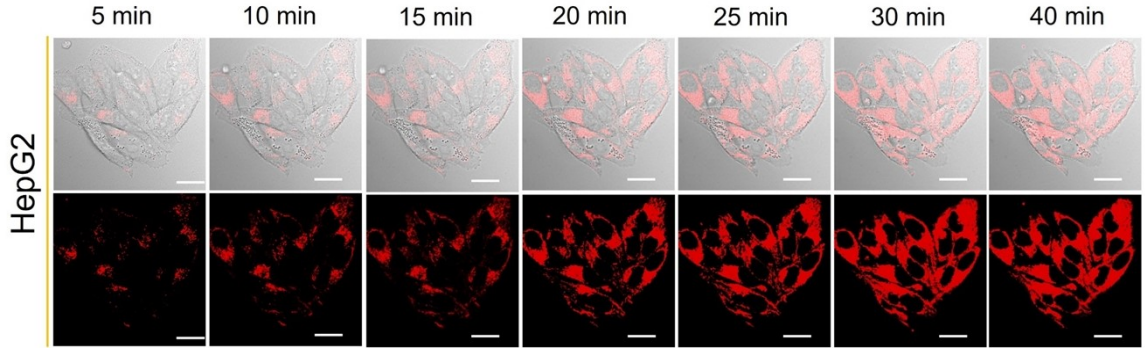

Fig. S11. Real-time imaging of endogenous GSH in HepG2 cells with HR-DX (5 μM). Fluorescent imaging in HepG2 cells incubated with HR-DX, the images were collected every 5 minutes. λ_{ex} =640 nm, λ_{em} =680-780 nm, scale bar: 20 μm.

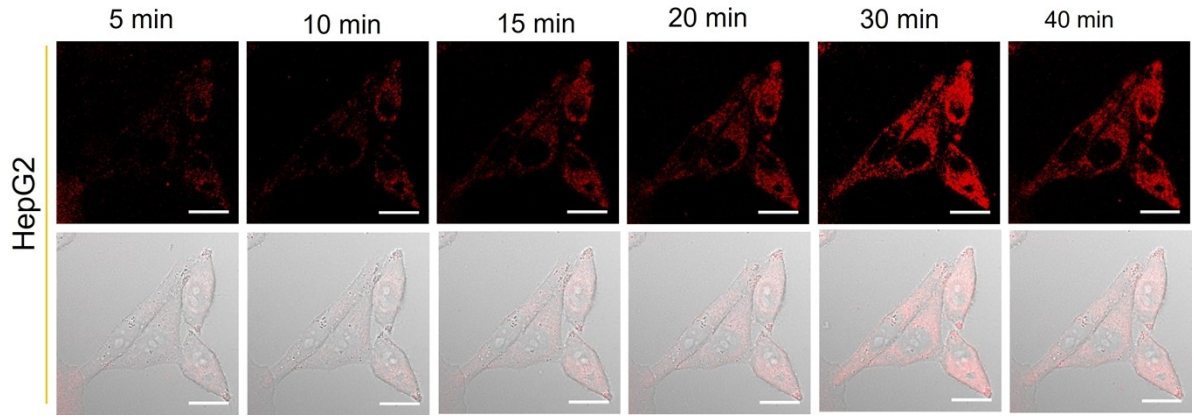

Fig. S12. Real-time imaging of endogenous GSH in HepG2 cells with HR-BX (5 μM). Fluorescent imaging in HepG2 cells incubated with HR-BX, the images were collected every 5 minutes. λ_{ex} =640 nm, λ_{em} =680-780 nm, scale bar: 20 μm.

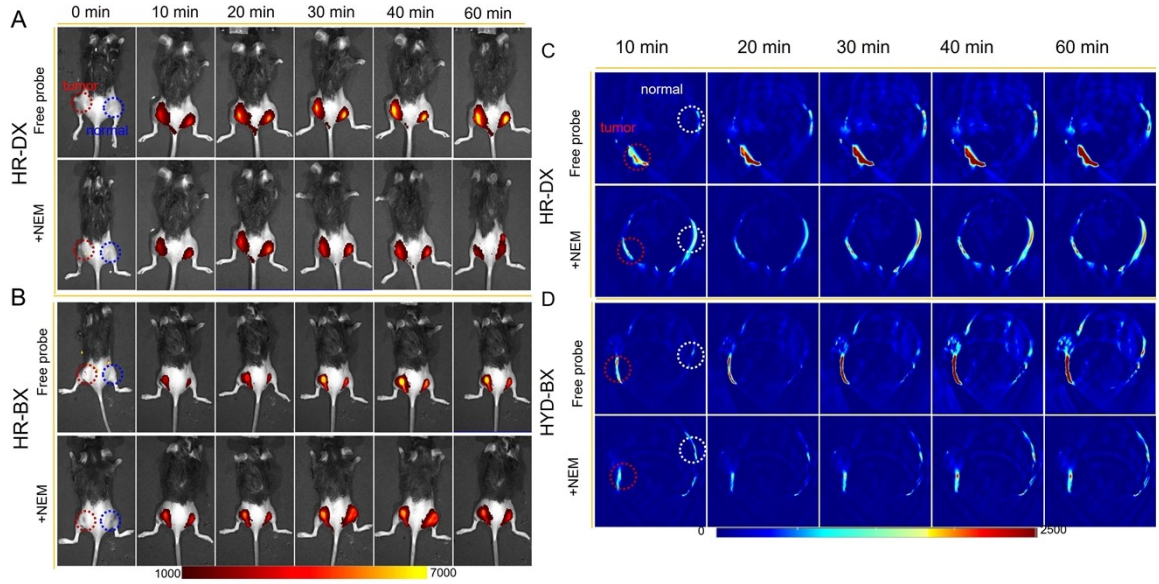

Fig. S13. In vivo NIR&PA fluorescent imaging of endogenous GSH or Cys in the A549-tumor-bearing mice with HR-DX or HR-BX (20 μM, 20 μL in DPBS/DMSO, v/v= 7:3, pH 7.4). (A and B) Real-time imaging in different groups of mice intra-tumoral injection of the probe, or pretreated with 5 mM NEM for 30 min then intra-tumoral injection of the probe. λ_{ex} =715 nm, λ_{em} =750-850 nm. (C and D) Real-time imaging in different groups of mice intra-tumoral injection of the probe, or pretreated with 5 mM NEM for 30 min then intra-tumoral injection of the probe; λ_{ex} = 735 nm for PA imaging.

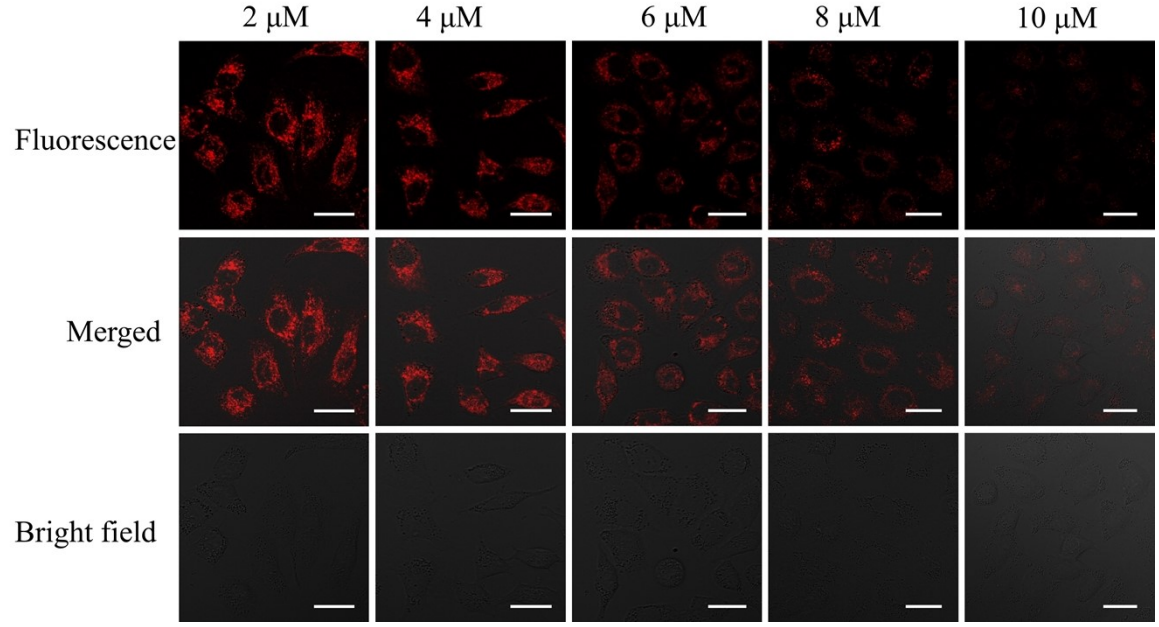

Fig. S14. Fluorescent imaging of A549 cells pretreated with different concertation of erastin (2-10 μM) for 4 h, before incubated with HR-DX (5 μM) for 30 min. λ_{ex} =640 nm, λ_{em} =680-780 nm, scale bar: 25 μm.

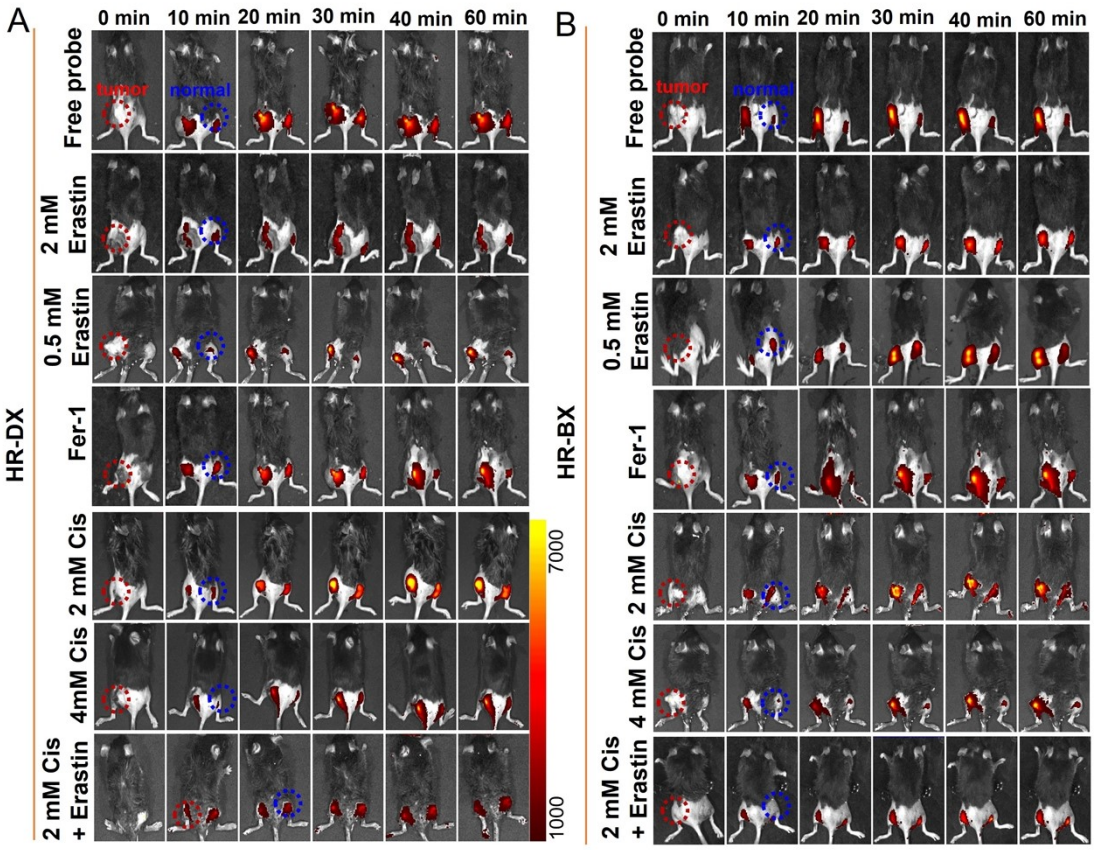

Fig. S15. *In vivo* NIR fluorescent of endogenous GSH and Cys during ferroptosis in the A549-tumor-bearing mice with HR-DX or HR-BX (20 μM, 25 μL in DPBS/DMSO, v/v= 7:3, pH 7.4). (A and B) Real-time fluorescent imaging in different groups of mice, from the first row to the seventh row: 1. intra-

tumoral injection of the probe only; 2. intra-tumoral pretreated with 2 mM erastin for 24 h then intra-tumoral injection of the probe; 3. intra-tumoral pretreated with 0.5 mM erastin for 24 h then intra-tumoral injection of the probe; 4. intra-tumoral pretreated with 2 mM erastin for 20 h followed with 2 mM Fer-1 for another 4 h then intra-tumoral injection of the probe; 5. intra-tumoral pretreated with 2 mM cisplatin for 24 h then intra-tumoral injection of the probe; 6. intra-tumoral pretreated with 4 mM cisplatin for 24 h then intra-tumoral injection of the probe; 7. intra-tumoral pretreated with 0.5 mM erastin and 2 mM cisplatin for 24 h then intra-tumoral injection of the probe; λ_{ex} =715 nm, λ_{em} =750-850 nm.

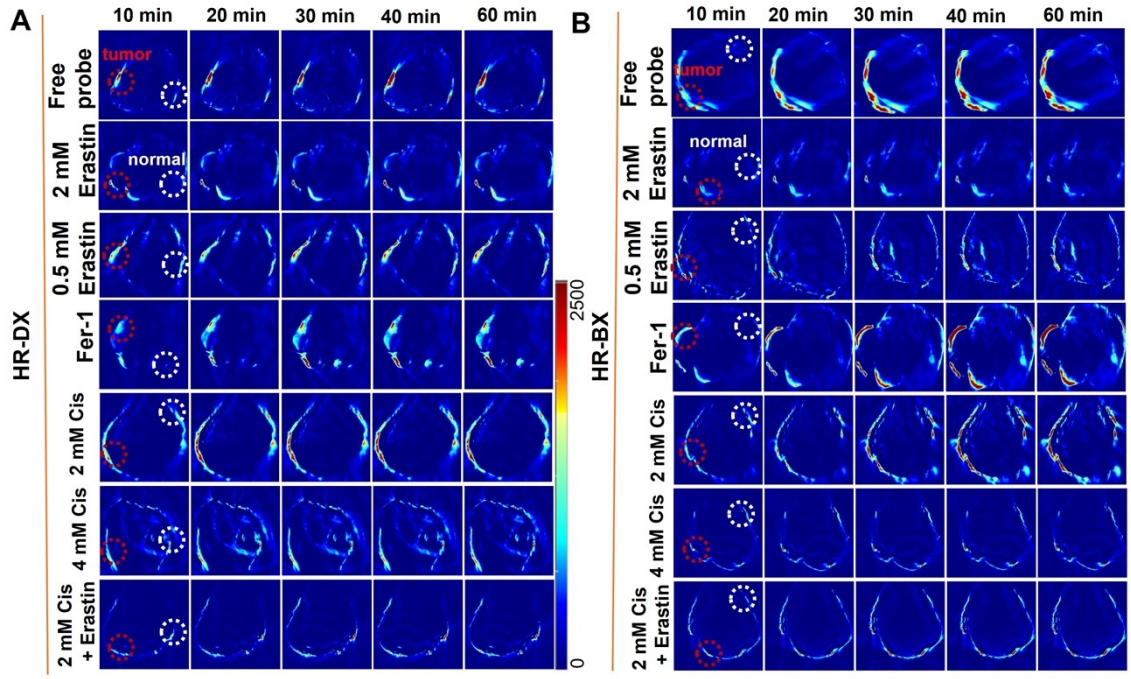

Fig. S16. *In vivo* PA imaging of endogenous GSH and Cys during ferroptosis in the A549-tumor-bearing mice with HR-DX or HR-BX (20 μM, 25 μL in DPBS/DMSO, v/v= 7:3, pH 7.4). (A and B) Real-time PA imaging in different groups of mice, from the first row to the seventh row: 1. intra-tumoral injection of the probe only; 2. intra-tumoral pretreated with 2 mM erastin for 24 h then intra-tumoral injection of the probe; 3. intra-tumoral pretreated with 0.5 mM erastin for 24 h then intra-tumoral injection of the probe; 4. intra-tumoral pretreated with 2 mM erastin for 20 h followed with 2 mM Fer-1 for another 4 h then intra-tumoral injection of the probe; 5. intra-tumoral pretreated with 2 mM cisplatin for 24 h then intra-tumoral injection of the probe; 6. intra-tumoral pretreated with 4 mM cisplatin for 24 h then intra-tumoral injection of the probe; 7. intra-tumoral pretreated with 0.5 mM erastin and 2 mM cisplatin for 24 h then intra-tumoral injection of the probe; λ_{ex} = 735 nm for PA imaging

3. Supplementary NMR and MS spectra

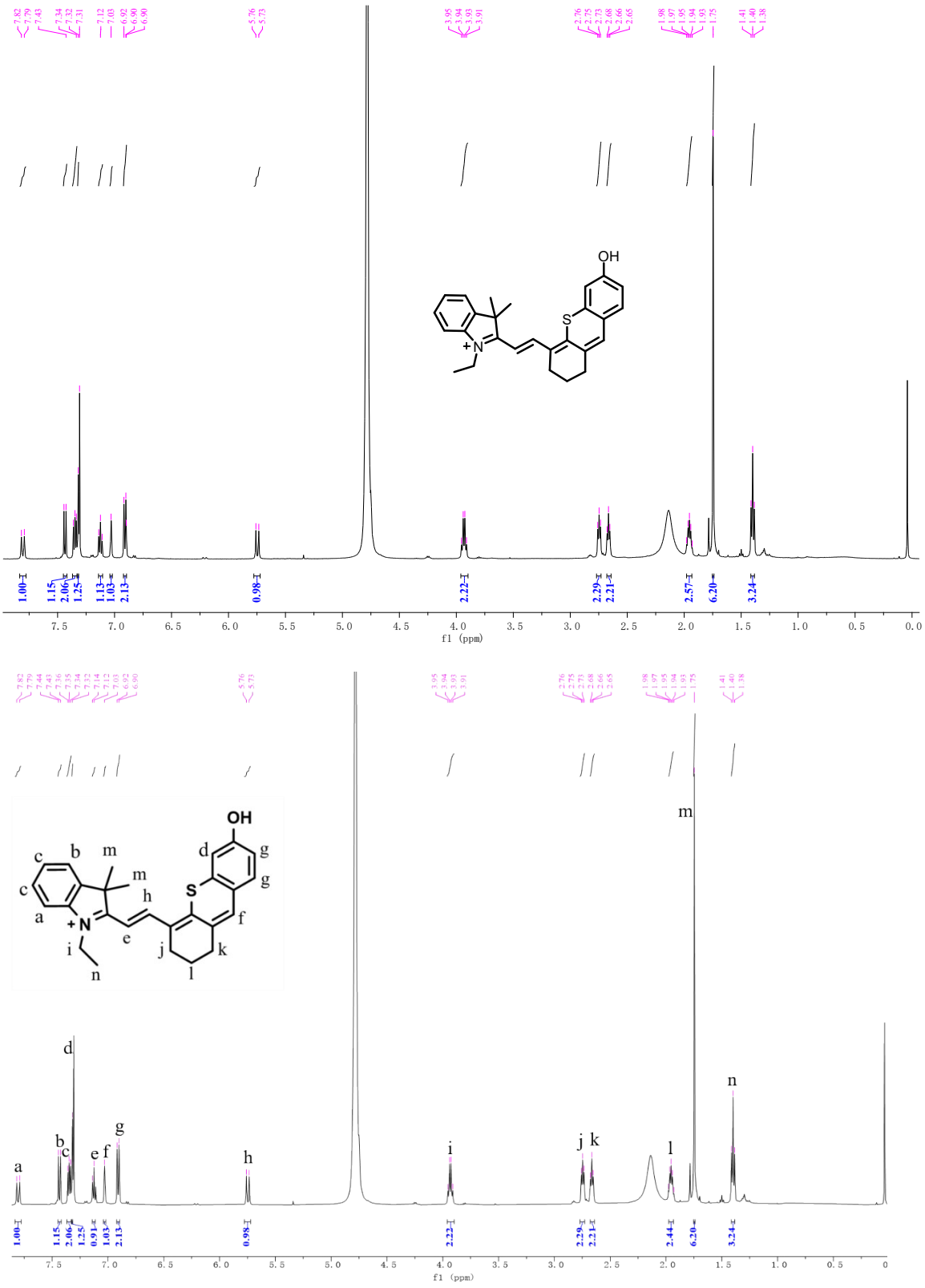

Fig. S17. ^{1}H NMR Spectrum of NIR dye **HR**.

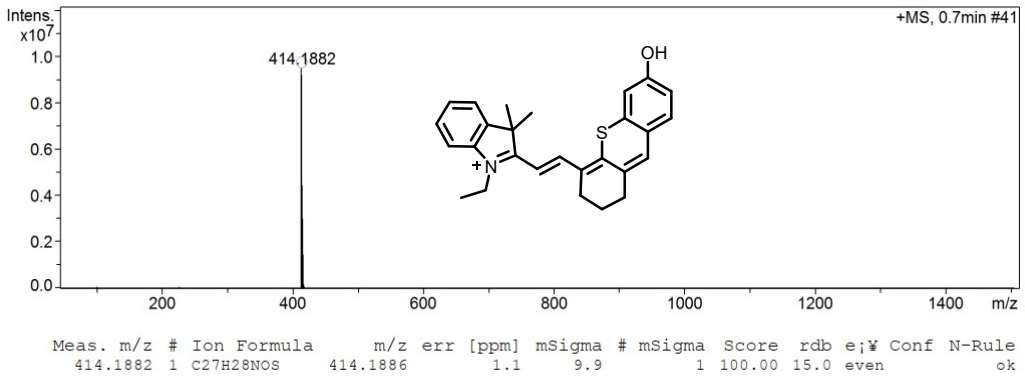

Fig. S18. ESI-HRMS Spectrum of NIR dye **HR**.

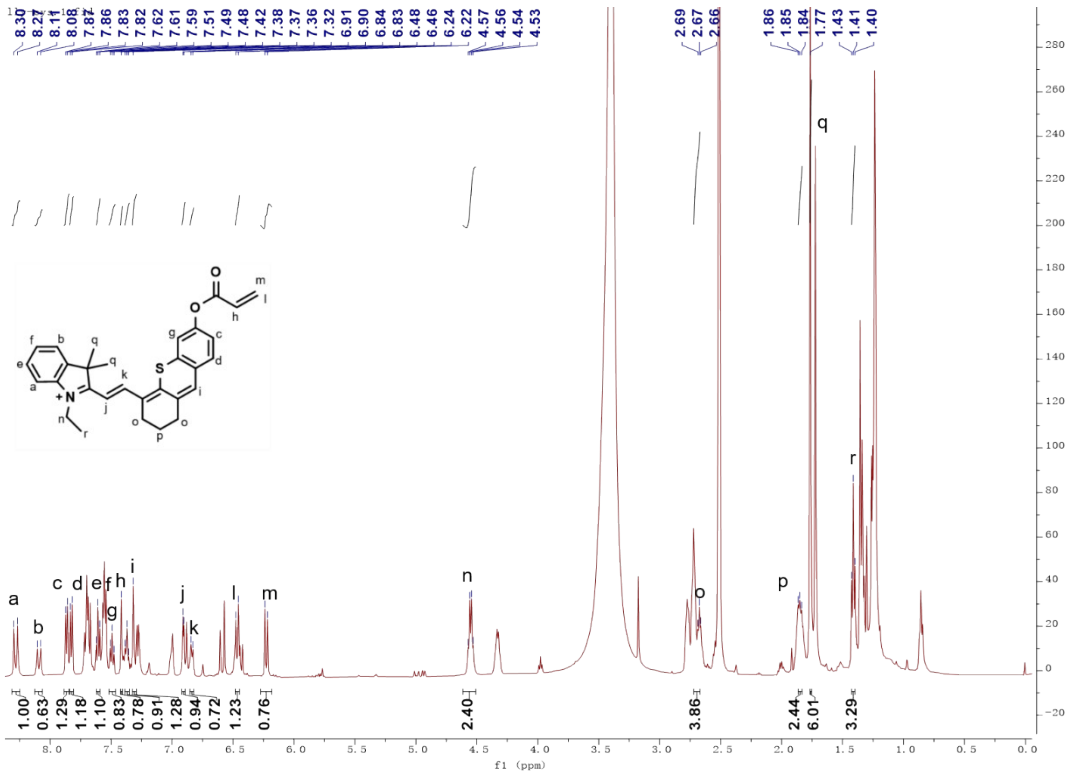

Fig. S19. ^{1}H NMR Spectrum of **HR-BX**.

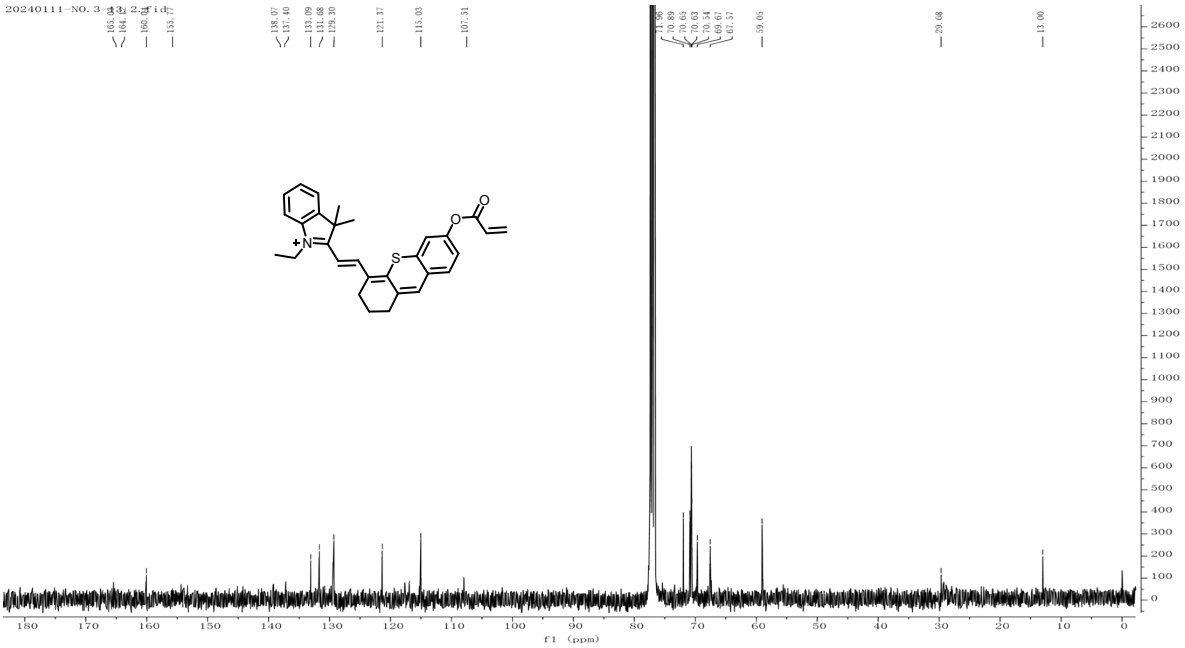

Fig. S20. ^{13}C NMR Spectrum of **HR-BX**.

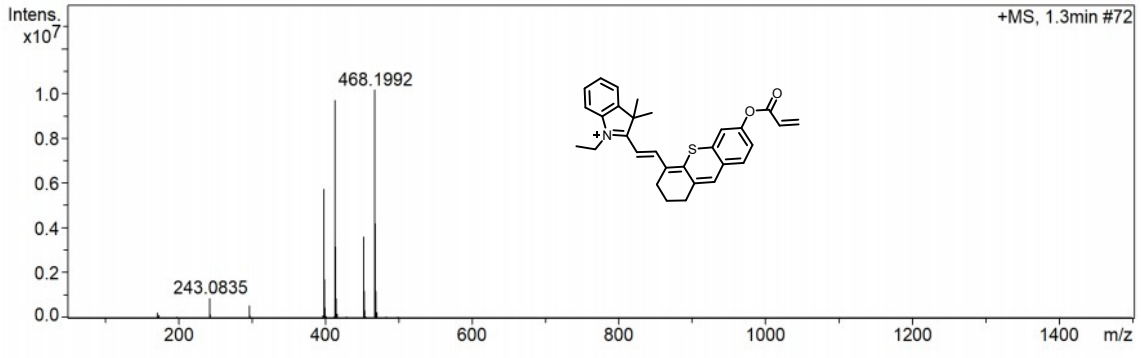

Fig. S21. ESI-Mass Spectrum of **HR-BX**.

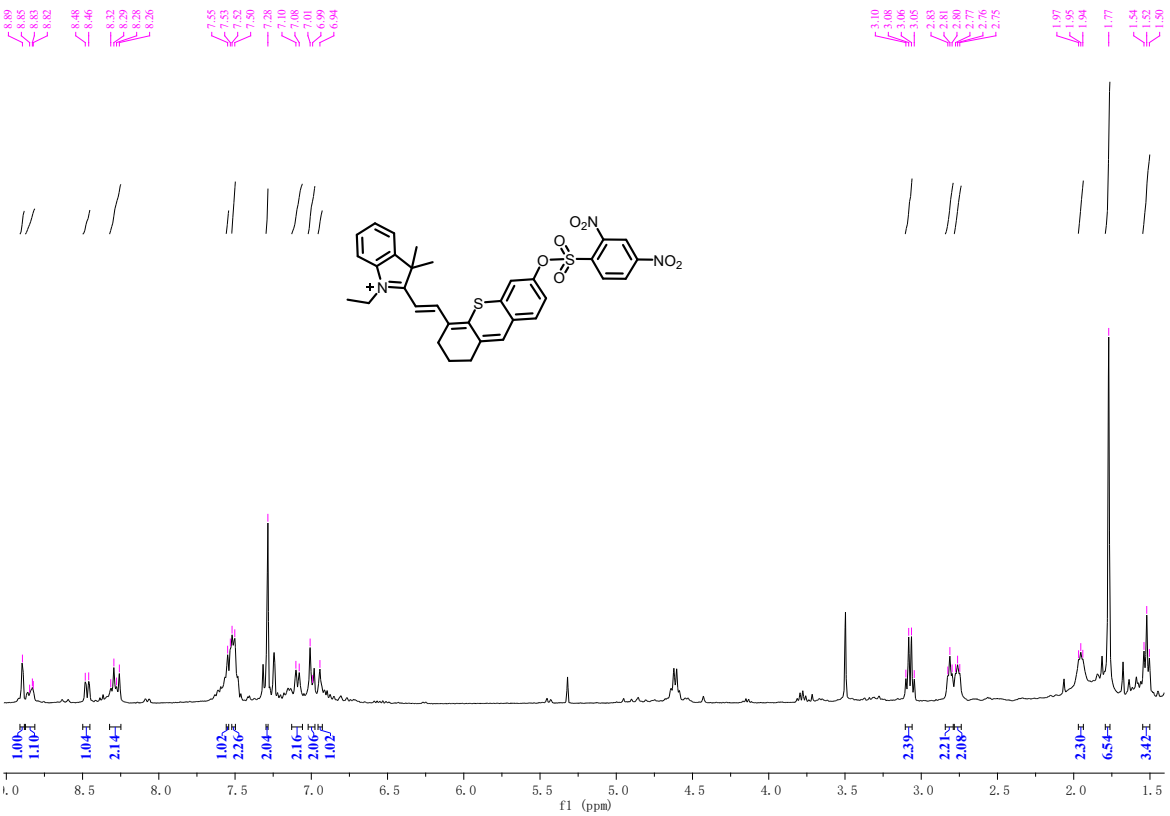

Fig. S22. [1]H NMR Spectrum of **HR-DX** in DMSO-d_6.

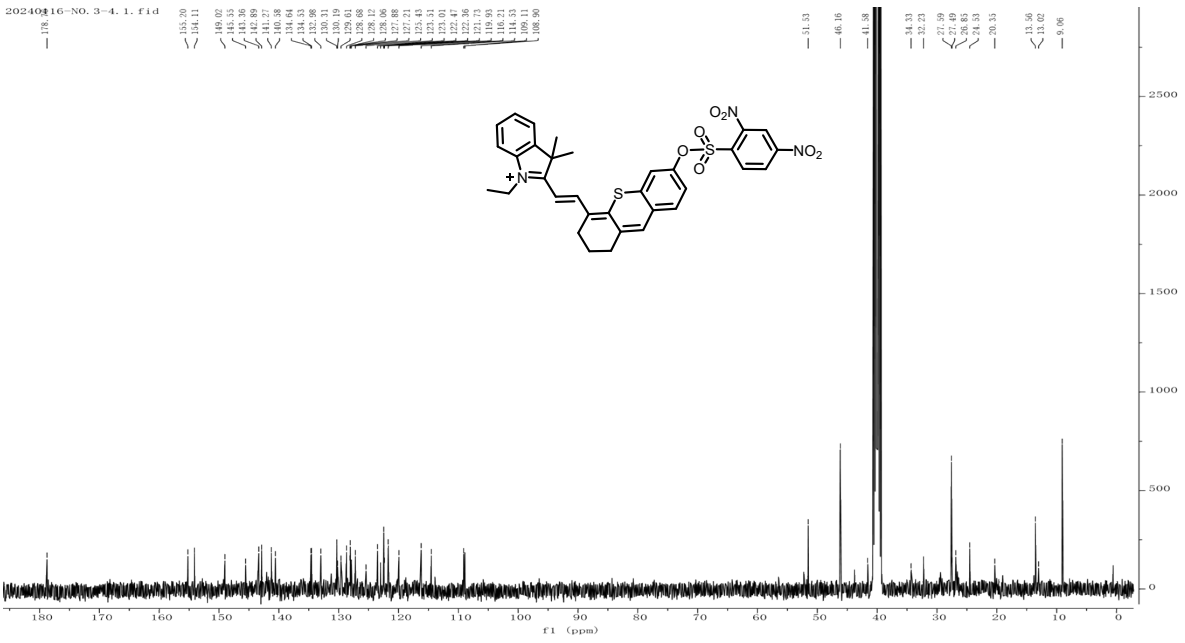

Fig. S23. [13]C NMR Spectrum of **HR-DX** in DMSO-d_6.

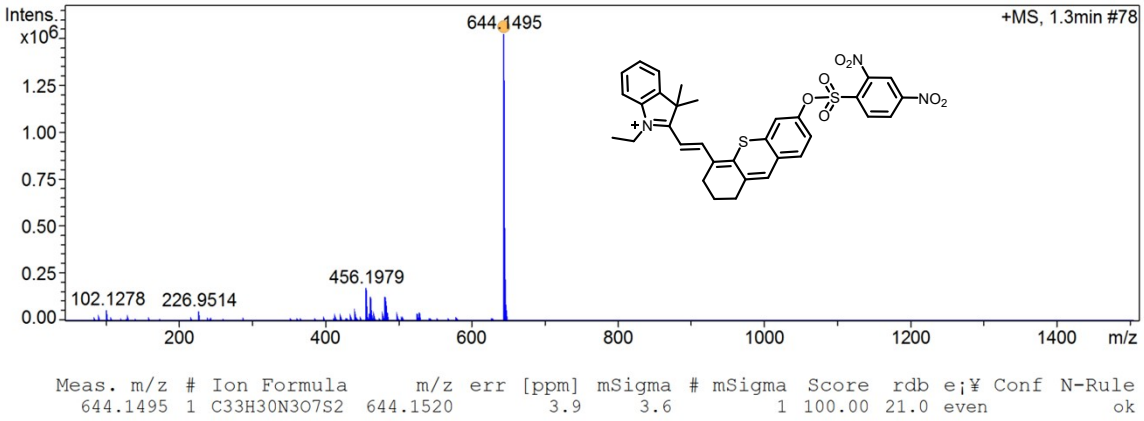

Meas. m/z	#	Ion Formula	m/z	err [ppm]	mSigma	# mSigma	Score	rdb	e¡¥	Conf	N-Rule
644.1495	1	C33H30N3O7S2	644.1520	3.9	3.6	1	100.00	21.0	even		ok

Fig. S24. ESI-HRMS Spectrum of **HR-DX**.